Research Article | Vol. 29, No. 20 / 27 Sep 2021 / Optics Express 30991
Optics EXPRESS

Experimental realization of integrated photonic reservoir computing for nonlinear fiber distortion compensation

STIJN SACKESYN,[1,2,*] CHONGHUAI MA,[1,2] JONI DAMBRE,[3] AND PETER BIENSTMAN[1,2]

[1] Photonics Research Group, Department of Information Technology, Ghent University - imec, Belgium
[2] Center for Nano- and Biophotonics (NB-Photonics), Ghent University, Belgium
[3] IDLab, Department of Information Technology, Ghent University - imec, Belgium
[*] stijn.sackesyn@ugent.be

Abstract: Nonlinearity mitigation in optical fiber networks is typically handled by electronic Digital Signal Processing (DSP) chips. Such DSP chips are costly, power-hungry and can introduce high latencies. Therefore, optical techniques are investigated which are more efficient in both power consumption and processing cost. One such a machine learning technique is optical reservoir computing, in which a photonic chip can be trained on certain tasks, with the potential advantages of higher speed, reduced power consumption and lower latency compared to its electronic counterparts. In this paper, experimental results are presented where nonlinear distortions in a 32 GBPS OOK signal are mitigated to below the 0.2×10^{-3} FEC limit using a photonic reservoir. Furthermore, the results of the reservoir chip are compared to a tapped delay line filter to clearly show that the system performs nonlinear equalisation.

1. Introduction

The ever-increasing drive for faster and denser communication in all aspects of the current digital society (video streaming, cloud services,. . .) keeps pushing the underlying optical technology forward at a high pace. One of the fundamental problems when data rates increase to even higher values in bandwidth-limited media is the Kerr effect in optical fibres. It can be responsible for multiple nonlinear optical effects, like self-phase modulation (SPM), cross-phase modulation (XPM) and four-wave mixing (FWM) [1]. In this paper, we will only handle single-wavelength signals, therefore only SPM will be of influence.

Several methods exist to correct for linear as well as nonlinear effects. The linear effects have been studied extensively in the past, and good-working solutions are established. Optical examples are dispersion compensating fibres and dispersion shifted fibres [2]. In the electrical domain, Tapped Delay Line filters (TDL) and Decision Feedback Equalisers (DFE) are widely used [3–5]. In terms of nonlinear impairment compensation, Digital Back Propagation (DBP) and nonlinear Volterra series are the most important electronic solutions, but both are power-hungry [6]. Important optical methods are Optical Phase Conjugation (OPC) and Phase-Conjugated Twin Wave (PC-TW) [7,8]. However, OPC will limit the system flexibility drastically as the link length needs to be known beforehand. PC-TW limits the spectral efficiency (SE) due to an additional twin wave that needs to be transmitted [9,10].

Numerous optical implementations of reservoir computing for optical signal processing applications have been investigated for over a decade now and can be divided into delayline-based reservoirs and spatially distributed reservoirs [11–16]. Reservoir computing was originally introduced as an efficient way to train a recurrent neural network [17,18], but it has caught a lot of attention as an easy-to-implement machine learning method in new hardware platforms. In reservoir computing, a recurrent neural network (RNN) is used as a means to enrich the feature

#435013 https://doi.org/10.1364/OE.435013
Journal © 2021 Received 6 Jul 2021; revised 27 Aug 2021; accepted 27 Aug 2021; published 13 Sep 2021

Optics EXPRESS

space of a given time series. This RNN is called the reservoir and will not be changed throughout the entire procedure. It can be modelled in a general form in discretized time using this state equation [19]:

$$\vec{x}[k+1] = f\left(\boldsymbol{W}_{res}\vec{x}[k] + \vec{w}_{in}(\vec{u}[k+1] + \vec{u}_{bias})\right) \tag{1}$$

where f is a nonlinear function, $\vec{u}$ is the input to the reservoir and $\vec{u}_{bias}$ is a fixed scalar bias applied to the inputs of the reservoir. For an N-node reservoir, $\boldsymbol{W_{res}}$ is an $N \times N$ matrix representing the interconnections between reservoir components. $\vec{w}_{in}$ is an N-dimensional column vector whose elements are nonzero for each active input node. The photonic reservoirs used in this work are purely passive, and thus no intrinsic nonlinearity is incorporated in the reservoir. All nonlinearity comes from the square nonlinear response of the photodetector when transforming the optical signal to the electronic domain. The training procedure only takes place in the readout stage, where the states of the nodes (or a subset thereof) will be linearly combined to match the desired output as closely as possible:

$$\vec{y}[k] = \vec{W}_{out} \cdot \vec{x}[k] \tag{2}$$

where $\vec{y}[k]$ is the output of the reservoir, and $\vec{W}_{out}$ are the respective weights for each state. Recently, different flavours of it have been investigated for applications in telecommunications specifically [20–23].

In this work, we will experimentally show for the first time that a waveguide-based photonic reservoir chip can compensate for linear as well as nonlinear impairments, without needing to slow down the input signal. Our approach processes the data in parallel by design and consequently has a very low latency cost. Furthermore, the equalization part of signal processing can be tackled in real time in the optical domain which keeps conversion to power-hungry electronics to a bare minimum. The rest of this paper is structured as follows. First, the design of the reservoir is discussed. Subsequently, we discuss the experimental setup that was used to perform the experimental measurements. Lastly, the results are presented in which our photonic reservoir is able to compensate below the Forward Error Correction (FEC) limit for the distortion induced by the combination of a nonlinearity-inducing amplifier and 25 km of optical fibre.

2. Photonic reservoir design

The design of this photonic reservoir is based on the four-port architecture which is a power-efficient evolution of the swirl architecture, by replacing all three-ports by four-ports [24]. The reservoir studied in this paper has 32 nodes in a 4 by 8 configuration as is shown in Fig. 1. The nodes that are used here are 3×3 MMIs which are in principle more symmetrical and more power efficient compared to other alternatives which use 1×2 and 2×1 MMIs. All signals are coupled to and from the chip by means of grating couplers. The chip can only be optically probed from 17 ports out of 32 nodes, which are distributed throughout the structure. The optical input signal is coupled to the chip at a single grating coupler and thereafter distributed on-chip through a tree of multimode interferometer (MMI) splitters to 10 nodes, enhancing the spatial uniformity of the power distribution in the reservoir structure. The signal is routed between nodes by photonic waveguides, for which the propagation delay of the signal travelling through one such connection corresponds to one bit period for all the inner waveguides. The outer waveguides have varying lengths, but are always chosen to be a multiple of one bit period. Simulations have shown that this delay strategy gives the best performance, since in that case the sampling points of the different delayed bit streams will be most optimally aligned. In addition, the longer delay lines at the outer side of the reservoir increase the intrinsic memory. They also break the symmetry within the reservoir which prevents it from having too similar outputs. As the length of the routing waveguides is inversely proportional to the bit period, the design can easily be adapted to faster bit rates to keep up with industry standards. The chip was fabricated in the SG25H4 SiGe BiCMOS technology platform from IHP technology [25], to operate at 1550 nm.

Optics EXPRESS

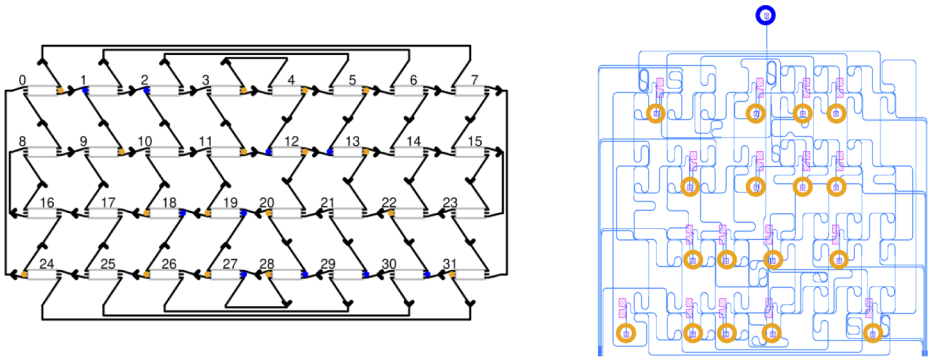

(a) (b)

Fig. 1. (a) Schematic drawing of the 32-node four-port reservoir. (b) Picture of the design on the level of the photonic structures. In (a), the input nodes are marked blue (1, 2, 12, 13, 18, 19, 27, 28, 29, 30). In (b), only the the main input grating coupler is indicated in blue. After this grating coupler, the signal is split and routed to the respective input nodes. The output nodes are marked orange (0, 3, 4, 5, 9, 11, 12, 13, 18, 19, 20, 22, 24, 26, 27, 28, 31) in both (a) and (b).

3. Experimental setup

The experiments presented in this paper are all done using a so-called electrical readout strategy. This means that the nodes are optically probed and detected by a photodiode one at a time. The signal is repeated in time entirely for each node to accomplish this. These electrical time traces are saved on a computer and the linear combination of these traces is done in post-processing on a computer. This is in contrast to a so-called optical readout strategy, where the optical signals are weighted and combined on-chip in the analogue optical domain, before being sent to a single photodiode. This latter method is certainly feasible, but has a higher technological complexity, which brings more challenges. The optical readout is subject to ongoing experiments and out of the scope of this paper. Long-term however, such a strategy is the way to go, as it can process the signals fully online, and only requires a single high-speed photodiode.

The experimental setup is shown in Fig. 2. Light at 1550 mm with a power level of 6.5dBm, generated by a commercial CW laser (Santec TSL-510) is modulated (Photline MX-LN-40) in a random stream of On-Off keyed bits at a rate of 32 Gigabit per second (GBPS). The modulator is biased in its linear region by driving it at $V_{bias} = 4.5V$. The random stream was generated by the Mersenne twister algorithm. Random signals with a simple generating rule like pseudorandom binary sequences (PRBS) are to be avoided, since in that case, the reservoir could take a shortcut and learn the generating rule, rather than being truly able to equalise arbitrary signals. This would lead to an overly optimistic performance estimate [26].

The signal is amplified (using a Keopsys CEFA-C-HG-SM-50-B201-FA-FA) and sent through a single-mode fibre of 25 km with an attenuation of 0.2dB/km at 1550nm. The amplifier in front of the fibre is an artificial means of increasing nonlinear distortion effects in the fibre and thus specifying the difficulty of the task to be solved by our reservoir computer. An amplifier after the fibre increases the optical power again to a set value which is the same for all experiments, irrespective of the power sent through the fibre. This ensures that the optical power that is sent through the reservoir is constant for all experiments, resulting in a fair way of comparing these tasks. Without this, the higher the power sent trough the fibre, the higher the power sent into the reservoir and the better the signal quality after detection after the reservoir, which would result in an unfair advantage of the nonlinear case over the linear case. Because of unexpected on-chip losses due to suboptimal design and fabrication of the MMIs, a third amplifier is needed

Optics EXPRESS

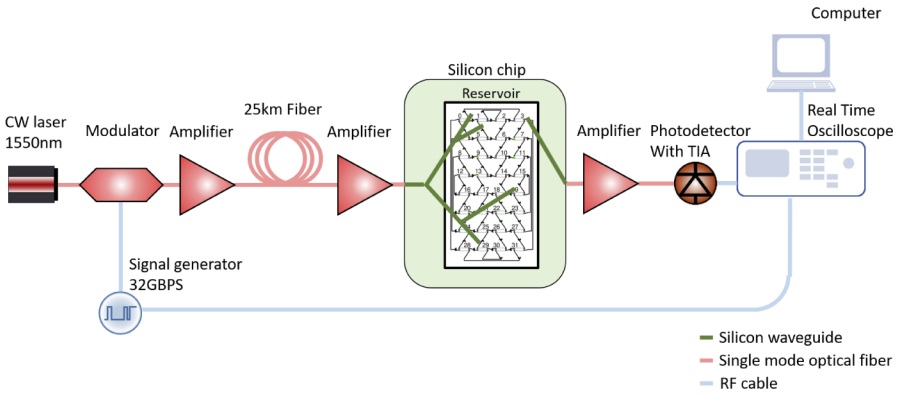

Fig. 2. Schematic illustration of the setup used in the experiment.

to amplify the signal to within the detection range of the photodetector. All amplifiers are the same Keopsys model which has a near quantum-limited noise figure of 4dB.

Finally, the signal is saved electronically and post-processed on a computer. The training of the weights consists mainly of a ridge regression algorithm [27] in which normalization is allowed. The labels used for training are the digital on-off keying bit stream. These electronic weights could have a much higher resolution than some non-volatile optical weights that could be used in an optical readout scheme. However, the effects of this limited weight resolution can be counteracted using specific algorithms [28].

The photonic reservoir will be compared to a Tapped Delay Line (TDL) filter, implemented digitally using the experimental time traces of the fibre output. For a fair comparison, the tapped filter should have the same number of degrees of freedom as the reservoir. Therefore, it is constructed by taking N copies - N is the number of probed reservoir nodes, i.e. 17 - of the distorted signal.

To compensate for timing uncertainties coming from the independent sequential measurements of the different channels, we temporally realign the channels by optimising the 17 time offsets using a Gaussian optimisation algorithm [29] which minimizes the BER. We look at two distinct cases. For the first case, the optimal time-offsets will be selected from a space which has a resolution of one bit: $t_i = t_0 + m \times T$ with $m \in \{-15, -14, \ldots, 15\}$, T the bit period and t_0 a global reference time for all channels, ensuring we sample in the middle of the bit period. We will refer to this as limited time-offset freedom. This corresponds best with how a real application would be configured, not wasting costly bandwidth on oversampling. In a second case, full time-offset freedom, the time offsets have a sub-bit-period resolution but with a smaller time range: $m \in \{-2.50, -2.45, \ldots, 2.50\}$. We do this to check if relative time offsets of less than a bit period could benefit the performance of the reservoir and/or that of the tapped delay line filter. In an integrated optical setup, such small time offsets do not necessarily need to result in a higher sampling rate, as these sub-bit-period offsets could be implemented using on-chip delay lines. In this way, also here a single sample per bit period would suffice.

After optimizing the time offsets, the N copies are linearly combined. Care was taken to ensure that this procedure is exactly the same both for the tapped filter and for the reservoir filter, so as to have a fair comparison.

4. Experimental results

The experiment was executed for three different levels of fibre distortion, provoked by driving the first amplifier to amplify to 10 dBm, 14 dBm and 18 dBm respectively. In Fig. 3, eye diagrams

Optics EXPRESS

are shown for the case where the random stream is amplified to 18 dBm of optical power and sent through the optical fibre. The Bit Error Rate (BER) of the uncorrected fibre output signal is 2.3×10^{-1} and the signal is visibly distorted in a nonlinear way.

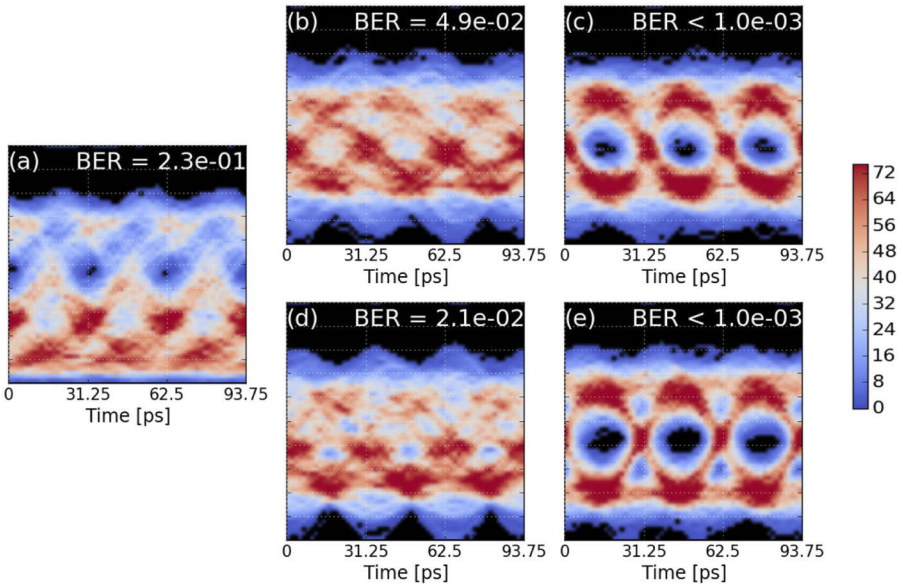

Fig. 3. Eye diagrams for the case of 18 dBm optical power insertion to the optical fibre. (a) The distorted signal. (b,d) The signal after a tapped delay line filter with (b) limited time-offset freedom and (d) full time-offset freedom. Similarly for (c,e) which are the signals after reservoir equalisation.

Let us first consider the case of limited time-offset freedom. The BER after a tapped delay line filter remains high at 4.9×10^{-2} (Fig. 3(b)). This indicates that for this power level, a considerable amount of nonlinear distortion is present. The BER retrieved after the reservoir chip is below the FEC limit (Fig. 3(c)), as 50 erroneous bits are picked up from the stream of 10^5 test bits. Note that this number of test bits limits the BER resolution to roughly 10^{-3}. A more precise number can not be reliably given with this test size [30], and scaling up the number of bits would mean a nontrivial change to the setup due to memory limitations of the signal generator, or switching to PRBS test signals.

We now switch to full time-offset freedom, and eye diagrams for those situations are shown in Fig. 3(d) and (e) for TDL and reservoir respectively. A TDL can reach a BER of 2.1×10^{-2}, still relatively high but lower than before. The reservoir achieves zero errors (although as before the statistically relevant BER resolution is 10^{-3}), and the eye diagram is visibly more open than previously for the limited time-offset freedom.

An overview of the performance of the reservoir compared to that of the tapped delay line filter is given in Fig. 4(a) for the three different amplifications of the signal and two different time-offset freedom cases. The BER of the tapped filter increases with increasing nonlinear distortion, which is to be expected. On the other hand, the reservoir can solve the task errorless within the measurement resolution for 10 dBm as well as for 14 dBm. For 18 dBm on the other hand, a BER of 5×10^{-4} is obtained for the limited time-offset freedom case, still below the 0.2×10^{-3} FEC limit. The reservoir is thus capable to correct for linear as well as for nonlinear fibre distortion effects. Potentially, electronic DSP will still be required in the pipeline. However, the complexity of the necessary DSP will decrease drastically as nonlinear compensation is the most demanding DSP sub-task, reducing power consumption and cost. When comparing the two

Optics EXPRESS

cases of time-offset freedom for the TDL, full freedom can indeed give a performance advantage. While counting errors at the 18 dBm level suggests that this could also apply for the reservoir, the current BER resolution of our measurements is not sufficient to draw statistically relevant conclusions.

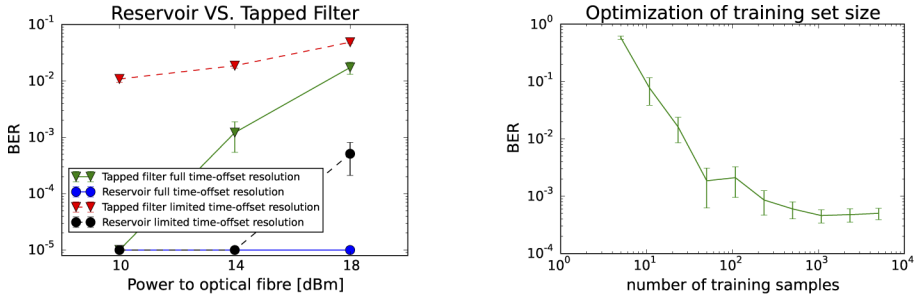

(a) (b)

Fig. 4. (a) The photonic reservoir equalizer in comparison to the tapped delay line filter. (b) BER for different training set sizes, all with a test size of 10^5 bits.

For application in a telecommunication system, it is important to have a feeling for the training set size. A too small training set would mean suboptimal performance, while if too many samples are considered during training, there will be an additional training time cost. Figure 4(b) shows the evolution of the BER for different training set sizes, for the 18 dBm case. The test set size is kept constant at 10^5, and five different test sets are used in a 5-fold cross validation scheme. The BER stops to improve at around 10^3 bits training set size, which is reasonably small. Note that this study considers training from scratch, i.e. without previous information. Periodic retraining to address drift in a real-life system could be more efficient using techniques that can take advantage of the knowledge of the previous set of weights.

5. Conclusion

This paper introduced the first experimental demonstration of nonlinear fibre distortion mitigation using a waveguide-based photonic reservoir, which is a real-time, integrated optics approach. We compared the reservoir to a tapped delay line filter for three types of distortion and two types of time-offset freedoms. The reservoir outperforms the linear baseline and stays overall below the 0.2×10^{-3} FEC limit for all cases. Further work will include implementing the linear combination on-chip in the optical domain.

Funding. EU H2020 Project Nebula (No. 871658);the EU project PHRESCO (H2020-ICT-2015-688579); Research Foundation Flanders (FWO) (1S32818N).

Disclosures. The authors declare no conflicts of interest.

Data availability. Data underlying the results presented in this paper are available upon reasonable request.

References

1. E. Ip and J. M. Kahn, "Compensation of dispersion and nonlinear impairments using digital backpropagation," J. Lightwave Technol. **26**(20), 3416–3425 (2008).
2. L. Gruner-Nielsen, M. Wandel, P. Kristensen, C. Jorgensen, L. Jorgensen, B. Edvold, B. Palsdottir, and D. Jakobsen, "Dispersion-compensating fibers," J. Lightwave Technol. **23**(11), 3566–3579 (2005).
3. E. Ip and J. M. Kahn, "Digital equalization of chromatic dispersion and polarization mode dispersion," J. Lightwave Technol. **25**(8), 2033–2043 (2007).
4. S. Tsukamoto, K. Katoh, and K. Kikuchi, "Unrepeated transmission of 20-Gb/s optical quadrature phase-shift-keying signal over 200-km standard single-mode fiber based on digital processing of homodyne-detected signal for group-velocity dispersion compensation," IEEE Photonics Technol. Lett. **18**(9), 1016–1018 (2006).

Optics EXPRESS

5. M. Taylor, "Coherent detection method using dsp for demodulation of signal and subsequent equalization of propagation impairments," IEEE Photonics Technol. Lett. **16**(2), 674–676 (2004).
6. J. C. Cartledge, F. P. Guiomar, F. R. Kschischang, G. Liga, and M. P. Yankov, "Digital signal processing for fiber nonlinearities," Opt. Express **25**(3), 1916–1936 (2017).
7. S. Le, M. McCarthy, S. K. Turitsyn, I. Phillips, D. Lavery, T. Xu, P. Bayvel, and A. Ellis, "Optical and digital phase conjugation techniques for fiber nonlinearity compensation," in *2015 Opto-Electronics and Communications Conference (OECC)*, (2015), pp. 1–3.
8. X. Liu, A. Chraplyvy, P. Winzer, R. Tkach, and S. Chandrasekhar, "Phase-conjugated twin waves for communication beyond the kerr nonlinearity limit," Nat. Photonics **7**(7), 560–568 (2013).
9. A. Abdelkerim, O. A. Dobre, R. Venkatesan, O. S. Sunish Kumar, P. Ciblat, and Y. Jaouën, "A survey on fiber nonlinearity compensation for 400 gb/s and beyond optical communication systems," IEEE Commun. Surv. Tutorials **19**(4), 3097–3113 (2017).
10. A. Katumba, X. Yin, J. Dambre, and P. Bienstman, "A neuromorphic silicon photonics nonlinear equalizer for optical communications with intensity modulation and direct detection," J. Lightwave Technol. **37**(10), 2232–2239 (2019).
11. G. Van der Sande, D. Brunner, and M. Soriano, "Advances in photonic reservoir computing," Nanophotonics **6**(3), 561–576 (2017).
12. H. Jaeger and H. Haas, "Harnessing nonlinearity: Predicting chaotic systems and saving energy in wireless communication," Science **304**(5667), 78–80 (2004).
13. Y. Paquot, J. Dambre, B. Schrauwen, M. Haelterman, and S. Massar, "Reservoir computing: A photonic neural network for information processing," Proc. SPIE **7728**, 77280B (2010).
14. L. Appeltant, M. Soriano, G. Van der Sande, J. Danckaert, S. Massar, J. Dambre, B. Schrauwen, C. Mirasso, and I. Fischer, "Information processing using a single dynamical node as complex system," Nat. Commun. **2**(1), 468 (2011).
15. K. Vandoorne, P. Mechet, T. Van Vaerenbergh, M. Fiers, G. Morthier, D. Verstraeten, B. Schrauwen, J. Dambre, and P. Bienstman, "experimental demonstration of reservoir computing on a silicon photonics chip," Nat. Commun. **5**(1), 3541 (2014).
16. D. Brunner and I. Fischer, "Reconfigurable semiconductor laser networks based on diffractive coupling," Opt. Lett. **40**(16), 3854–3857 (2015).
17. M. Lukoševičius and H. Jaeger, "Reservoir computing approaches to recurrent neural network training," Comp. Sci. Rev. **3**(3), 127–149 (2009).
18. W. Maass, T. Natschläger, and H. Markram, "Real-time computing without stable states: A new framework for neural computation based on perturbations," Neural Comput. **14**(11), 2531–2560 (2002).
19. A. Lugnan, A. Katumba, F. Laporte, M. Freiberger, S. Sackesyn, C. Ma, E. Gooskens, J. Dambre, and P. Bienstman, "Photonic neuromorphic information processing and reservoir computing," APL Photonics **5**(2), 020901 (2020).
20. S. Wang, N. Fang, and L. Wang, "Signal recovery based on optoelectronic reservoir computing for high speed optical fiber communication system," Opt. Commun. **495**, 127082 (2021).
21. S. Magalhães Ranzini, R. Dischler, F. Da Ros, H. Bülow, and D. Zibar, "Experimental demonstration of optoelectronic equalization for short-reach transmission with reservoir computing," in *Proceedings of 46th European Conference on Optical Communication*, (IEEE, 2020).
22. A. Argyris, J. Bueno, and I. Fischer, "Photonic machine learning implementation for signal recovery in optical communications," Sci. Rep. **8**(1), 8487 (2018).
23. M. Sorokina, S. Sergeyev, and S. Turitsyn, "Fiber-optic reservoir computing for qam-signal processing," in *2018 European Conference on Optical Communication (ECOC)*, (2018), pp. 1–3.
24. S. Sackesyn, C. Ma, A. Katumba, J. Dambre, and P. Bienstman, "A power-efficient architecture for on-chip reservoir computing," in *Artificial neural networks and machine learning–ICANN 2019 : workshop and special sessions*, vol. 11731 (Springer, 2019), pp. 161–164.
25. D. Knoll, S. Lischke, A. Awny, and L. Zimmermann, "(invited) SiGe BiCMOS for optoelectronics," ECS Trans. **75**(8), 121–139 (2016).
26. T. A. Eriksson, H. Bülow, and A. Leven, "Applying neural networks in optical communication systems: Possible pitfalls," IEEE Photonics Technol. Lett. **29**(23), 2091–2094 (2017).
27. F. Pedregosa, G. Varoquaux, A. Gramfort, V. Michel, B. Thirion, O. Grisel, M. Blondel, P. Prettenhofer, R. Weiss, V. Dubourg, J. Vanderplas, A. Passos, D. Cournapeau, M. Brucher, M. Perrot, and E. Duchesnay, "Scikit-learn: Machine learning in Python," Journal of Machine Learning Research **12**(85), 2825–2830 (2011).
28. C. Ma, F. Laporte, J. Dambre, and P. Bienstman, "Addressing limited weight resolution in a fully optical neuromorphic reservoir computing readout," Sci. Rep. **11**(1), 3102 (2021).
29. J. Bergstra, D. Yamins, and D. D. Cox, "Making a science of model search: Hyperparameter optimization in hundreds of dimensions for vision architectures," in *Proc. of the 30th International Conference on Machine Learning* (ICML 2013), (2013).
30. M. Jeruchim, "Techniques for estimating the bit error rate in the simulation of digital communication systems," IEEE J. Select. Areas Commun. **2**(1), 153–170 (1984).